SOILS AND FOUNDATIONS Vol. 27, No. 1, 14-22, Mar. 1987 Japanese Society of Soil Mechanics and Foundation Engineering

# HYDROFRACTURING PRESSURE OF COHESIVE SOILS

AKIRA MORI\* and MASAHITO TAMURA\*\*

#### ABSTRACT

Investigated is the relation between the hydrofracturing pressure  $P_f$  and the strength of cohesive soils. Fracture tests on six kinds of cohesive soils (i.e.  $\phi=0$  materials), including artificial soils, were performed. The direction of fracture surface was chosen not only vertical (i.e. parallel to the borehole) but also horizontal and inclined. The result is the following equation in terms of total stress.

$$P_f = \sigma_{\min} + q_u$$

 $\sigma_{\min}$ : the minimum principal stress,  $q_u$ : the unconfined compression strength The shear failure—rather than the tensile failure—near the borehole initiates the hydrofracture of cohesive soils. This fracture mechanism seems to be reasonable, especially in case of the horizontal or inclined fracture. The viscosity of liquid in the borehole, the sample size and the pre-existent crack around the borehole have little influence on the fracturing pressure as far as the pressurizing rate is high enough to prevent the liquid to penetrate into the wedge.

Key words: cohesive soil, failure, grouting, laboratory test (IGC: K2/D6)

#### INTRODUCTION

Since Bjerrum et al (1972) had indicated the effect of hydraulic fracture in estimating the in-situ permeability, the hydraulic fracture becomes more important in soil engineering. Massarsch and Broms (1977) had pointed out the fracture phenomenon caused by pile driving in clay. Morgenstern and Vaughan (1963) had studied the allowable grouting pressures in permeable ground.

The grouting for cohesive soils is completely different from that for cohesionless soils since the chemical grout can not permeat and the hydraulic fracture occurs in all cases. After the chemical grout injected by fracturing into the cohesive soils is solidified, the strength is originated structurally by the flat solidified grout in the soil mass. The structural strength is deeply related to the circumstances of fracture. Therefore, it is important to clarify the fracture mechanism, including the vertical fracture and the horizontal or inclined fracture, in connection with the pressure required to arise the hydrofracture, the confining stress, and the strength of cohesive soils.

In the fileds of rock mechanics, for the

- \* Professor, Department of Civil Engineering, Waseda Univ., Shinjuku-ku, Tokyo.
- \*\* Graduate Student of Waseda Univ., Shinjuku-ku, Tokyo.

  Manuscript was received for review on March 20, 1986.

  Written discussions on this paper should be submitted before October 1, 1987, to the Japanese Society of Soil Mechanics and Foundation Engineering, Sugayama Bldg. 4F, Kanda Awaji-cho 2-23, Chiyoda-ku, Tokyo 101, Japan. Upon request the closing date may be extended one month.

purpose of determining the in-situ tectonic stress and moreover in petroleum industry, many papers had been reported about the hydraulic fracture. Hubbert and Willis (1957) had investigated theoretically the hydraulic fracture of the penetrating and non-penetrating type. Haimson and Fairhurt (1967, 1970) had found through the fracture tests on many kinds of rocks that the hydrofracturing pressure  $P_f$  can be given by Eq. (1) or Eq. (2) under three dimensional stress condition.

permeable type

$$P_{f}-P_{0}=\frac{3\sigma_{2}-\sigma_{3}+\sigma_{t}}{2-\alpha\lceil(1-2\nu)/(1-\nu)\rceil} \quad (1)$$

impermeable type

$$P_f - P_0 = 3\sigma_2 - \sigma_3 + \sigma_t \tag{2}$$

 $\sigma_2$ : the intermediate effective principal stress

 $\sigma_3$ : the minimum effective principal stress

 $\sigma_t$ : the effective tensile strength

 $\nu$ : the poissons ratio

 $\alpha$ : the porus-elastic parameter

$$\alpha = 1 - (C_r/C_b)$$

 $C_r$ =material matrix compressibility

 $C_b$  = material bulk compressibility

P<sub>0</sub>: the pore water pressure at a great distance from the borehole

However, it had been demonstrated that  $\sigma_t$  used in Eqs. (1) and (2) was larger than  $\sigma_t$  determined in Brazilian tests on the rock or concrete and that the hydrofracturing pressure would be influenced by the pressurizing rate and the viscosity of the liquid in the borehole (i.e. the degree of liquid permeation). (Zoback et al, 1977; Ishizima et al, 1980; Harada et al, 1985). Thus it is difficult to determine the hydrofracturing pressure prior to the fracture test. Lockner and Byerlee (1977) had pointed out that the hydrofracture could be initiated not only by the tensile failure but also by the shear failure at high confining pressure and differential stress.

Jaworski et al (1982) had performed the fracture tests on compacted soils to investigate the failure of Teton Dam and found that the hydrofracturing pressure  $P_f$  was

given by Eq. (3) which was originally derived by Vaughan (1971).

$$P_f = m\sigma_h + \sigma_{ta} \tag{3}$$

m: the slope of the linear function of fracturing pressure with horizontal stress

 $\sigma_{ta}$ : the apparent tensile strength

And they had pointed out that  $\sigma_{ta}$  was much larger than  $\sigma_t$  determined in Brazilian tests and that the maximum value of  $P_f$  would become the pressure required to initiate the cavity expansion.

The object of this study is to elucidate the mechanism of fracture initiation, especially the value of apparent tensile strength  $\sigma_{ta}$ . The reason why  $\sigma_{ta}$  is "apparent" is that the failure mechanism by hydrofracturing might be different from the tensile failure by the uniaxial tensile test or the Brazilian test. In experiment, the fracture tests on six kinds of cohesive soils (i. e.  $\phi = 0$  materials) were performed.

# SAMPLES AND TEST PROCEDURE

Table 1 shows the mechanical property of the test samples. The tensile strength  $\sigma_t$  was determined in Brazilian tests. Fig. 1 shows the stress-strain behaviour of samples in the unconfined compression tests. Fig. 2 shows the test results of unconsolidated un-

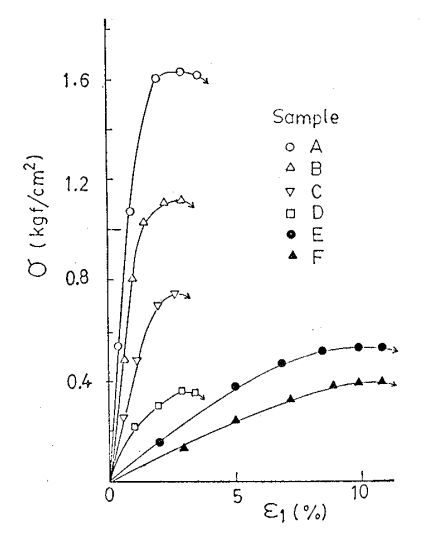


Fig. 1. Unconfined compression tests: 1kgf/cm<sup>2</sup>=98kN/m<sup>2</sup>

Table 1. Test samples

Sample No.	Components	$q_u = (\text{kgf/cm}^2)$	$\sigma_t$ (kgf/cm <sup>2</sup> )	$ ho_t$ (gf/cm <sup>3</sup> )	w (%)	w <sub>L</sub> (%)	w <sub>P</sub> (%)
A	Kibushi clay 2400, Bentonite 300, Gypsum 1100, Water 1800 (gram)	1.40~1.80	0.32~0.35	1.78	56	80	31
В	Kibushi clay 2400, Bentonite 300, Gypsum 1000, Water 1800 (gram)	1.00~1.30	0.21~0.24	1.63	57	79	28
. <b>C</b>	Kibushi clay 2400, Bentonite 300, Gypsum 750, Water 1700 (gram)	0.75~0.83		1.61	59	79	26
D	Kibushi clay 2400, Bentonite 300, Gypsum 500, Water 1600 (gram)	0.32~0.38		1.66	59	68	22
E	Consolidated Kaolin clay p <sub>c</sub> =3.00kgf/cm <sup>2</sup>	0.50~0.57		1.75	38	47	30
F	Consolidated Kaolin clay $p_c$ =2.00kgf/cm <sup>2</sup>	0.35~0.41		1. 74	40	47	30

Sample A, B, C and D were mixed clays and not consolidated.  $p_c$ : Preconsolidation pressure  $1 \text{kgf/cm}^2 = 98 \text{kPa}$  of sample C, D, E and F could not be determined in Brazilian tests.

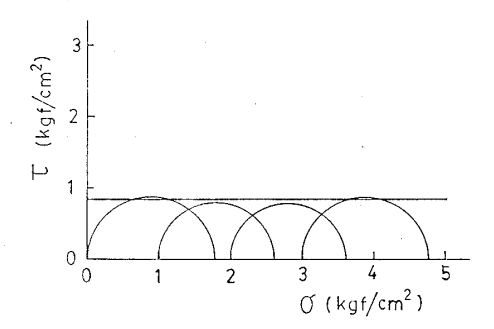


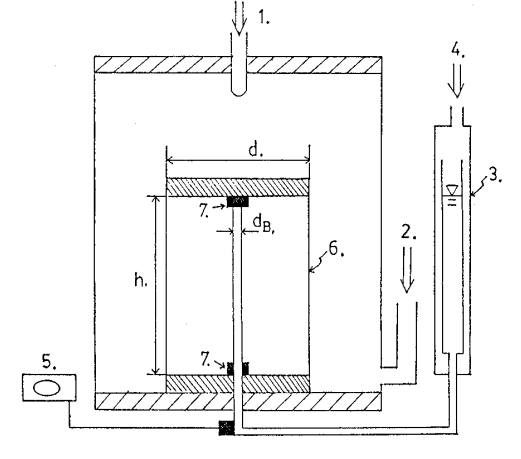
Fig. 2. Unconsolidated undrained test of sample A

drained triaxial compression test in the case of sample A.  $\phi_U$  of all samples were equal to zero.

Sample A, B, C, and D were the artificially prepared cohesive soils composed of Kibushi clay, bentonite, gypsum and water. They were mixed in the desired proportion and covered with vinyl sheet for one day to prevent the desiccation. Sample E and F were the kaolin clay consolidated under the pressure of 2.00 and 3.00 (kgf/cm²) respectively. All sample were cut down in the desired size from the soil mass and were not consolidated in the fracturing apparatus.

The sample size is  $75 \,\mathrm{mm}$  (=d: diameter of the specimen) and  $4 \,\mathrm{mm}$  (= $d_B$ : diameter of the borehole) in most cases. When the tests to investigate the effect of the sample size on the hydrofracturing pressure were performed, the samples of three different d (50, 75 and 150 mm) and two different  $d_B$  (4 and 8 mm) were chosen.

Fig. 3 shows the schematic diagram of frac-



1: Deviator stress

2: Lateral pressure

3: Burette

4: Borehole pressure

5: Pressuremeter

6: Specimen

7: Plastic gum

d: diameter of sample

 $d_B$ : diameter of borehole

h: height of sample (=[1.0 $\sim$ 2.0]·d)

Fig. 3. Triaxial fracturing apparatus

turing apparatus. After the borehole was filled with the liquid, the plastic gum was packed at the upper end of borehole to prevent the leakage of liquid. The impermeable grease layer was formed at both ends of the specimen. To prevent the borehole to be broken by the lateral pressure under the zero borehole pressure, the lateral pressure was applied stepwise at the same time with the borehole pressure P. The lateral pressure was kept constant during the fracture test. The pressurizing rate of the borehole pressure  $P_r$  was  $0.02 \, (kgf/cm^2/s)$  in most

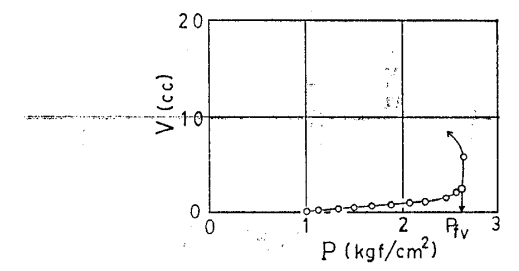


Fig. 4. Relation between inflow volume V and borehole pressure P (Sample A,  $\sigma_h=1.00 \, \text{kgf/cm}^2$ , 1 (cp) liquid)

cases. The effect of the deviator stress on the vertical hydrofracturing pressure was small. The deviator stress was  $20\sim30\%$  of the unconfined compression strength  $q_u$  of sample in vertical fracture tests.

The fracture initiation was detected by monitoring the inflow volume V measured by the burette. Fig. 4 shows the typical result of the relation between the borehole pressure P measured by the pressuremeter and the inflow volume V. The sudden increase of inflow volume was accompanied by the decrease of borehole pressure. This is probably due to the penetration of the liquid into the cracks around the borehole caused by hydrofracturing.

In horizontal or inclined fracture tests, the triaxial apparatus, where the axial pressure could be applied independently irrespective of the lateral pressure, was used. After taking out the fractured specimen from the apparatus, the liquid colored by Rhodamine B was slowly injected into the borehole. The direction of fracture was determined by the state of liquid penetration after cutting down the specimen. In vertical fracture, the crack near the borehole was developed in the radial straight way. On the other hand, in the horizontal or inclined fracture, the crack was not straight and it was difficult to see whether the crack was horizontal or inclined clearly.

# VERTICAL HYDROFRACTURE

Fig. 5 shows the test results of sample A. It can be seen from Fig. 5 that the effect of the viscosity of the liquid in the

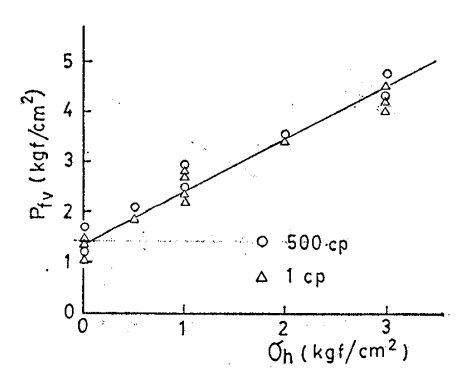


Fig. 5. Vertical fracture tests of sample  $A: 1 kgf/cm^2 = 98 kN/m^2$ 

borehole on the hydrofracturing pressure was small, for the vertical hydrofracturing pressure  $P_{fv}$  with 1 (cp) liquid was almost equal to the hydrofracturing pressure with 500 (cp) liquid. The viscosity of liquid was adjusted by Sodium Carboxymethyl Cellulose.

The relation between the vertical hydro-fracturing pressure  $P_{fv}$  and the lateral pressure  $\sigma_h$  is given by Eq. (4).

$$P_{fv} = \sigma_h + \sigma_{ta} = \sigma_h + q_u \tag{4}$$

 $\sigma_{ta}$ : the apparent tensile strength

Although the circumferential total stress around the borehole is not negative when P becomes larger than  $\sigma_h$ , the tensile stress would be mobilized effectively when  $P > \sigma_h$  (i. e. the decrease of effective tangential normal stress), because all tests were performed in unconsolidated condition.

The  $\sigma_{ta}$  is a little smaller than the unconfined compression strength  $q_u$  of the sample A, for the value of  $q_u$  is 1.40~1.80 (kgf/cm<sup>2</sup>).

Figs. 6, 7 and 8 show the test results with

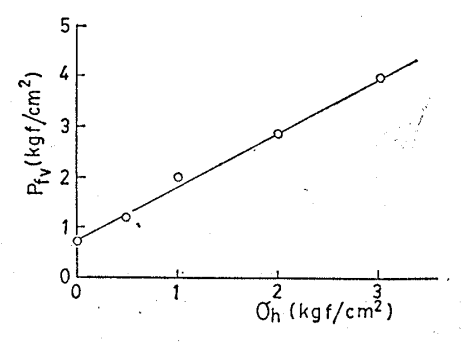


Fig. 6. Vertical fracture tests of sample C:500 (cp) liquid

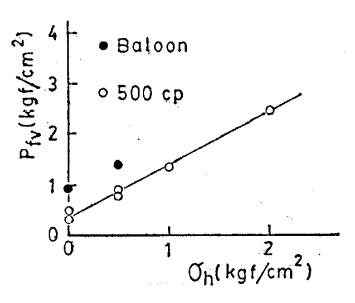


Fig. 7. Vertical fracture tests of sample D: 500 (cp) liquid

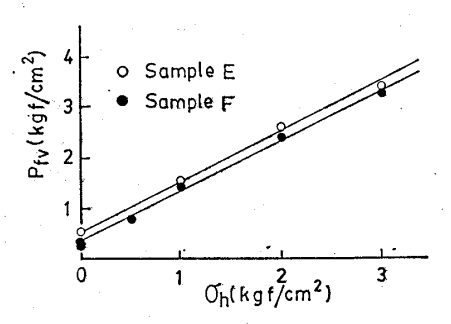


Fig. 8. Vertical fracture tests of sample E and F: 500 (cp) liquid

sample C, D, E and F. It is found from these results that Eq. (4) can be applied to the results and that  $\sigma_{ta}$  is almost equal to the unconfined strength of these samples.

The solid circle in Fig. 7 presents the fracturing pressure given by the balloon instead of the liquid. The fracturing pressure by the balloon is much larger than  $P_{fv}$  by the liquid. Table 2 shows the relation between the cavity expansion pressure  $P_u$  suggested by Vesic (1972) or Massarsch (1978) as well as the fracturing pressure given by the balloon. Table 2 indicates that the fracturing pressure by the balloon was almost equal to  $P_u$ . Thus the hydrofracturing pressure might become  $P_u$  when the viscosity of the

Table 2. Fracturing pressure  $P_f$  by the balloon

lateral stress (kgf/cm²)	fractuing pressure (kgf/cm²)	cavity expansion pressure $P_u(\text{kgf/cm}^2)$			
$\sigma_h$	$P_f$	$P_{u1}$	$P_{u2}$		
0.5	0.90	0.83~0.99	0.83~0.99		
1.0	1.35	1.33~1.49	1.33~1.49		

$$\begin{split} &P_{u1} = C \cdot [\ln\{E/2\,C(1+\nu)\} + 1] + \sigma_h \text{ (Vesic, 1972)} \\ &P_{u2} = C \cdot \ln[1.36\,E/C(1+\nu)] + \sigma_h \text{ (Massarsch, 1978)} \\ &(C = q_u/2, E = 100 \cdot q_u, \nu = 0.50, q_u = 0.32 \sim 0.38 \text{kgf/cm}^2: \\ &1 \text{kgf/cm}^2 = 98 \text{ kN/m}^2) \end{split}$$

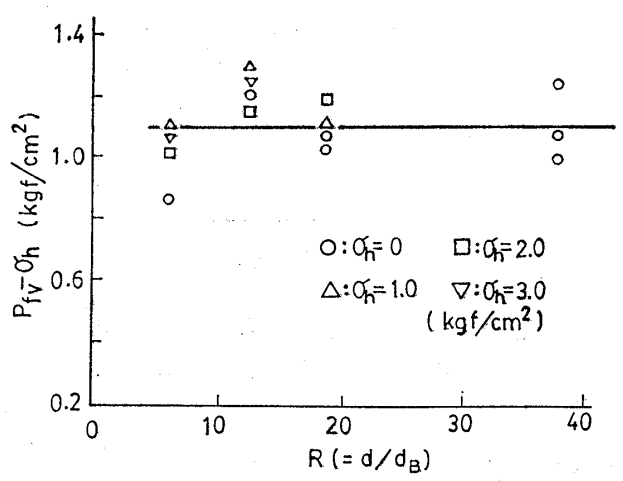


Fig. 9. Effect of the sample size on the hydrofacturing pressure  $P_{fv}$  of sample B:500 (cp) liquid

liquid were remarkably high. However, the pressure given by Eq. (4) rather than the cavity expansion pressure  $P_u$  as the hydrofracturing pressure in engineering practice would be chosen, because the viscosity of the grout is not high enough generally.

Fig. 9 shows the results with sample B. In these tests, the effect of the size of sample on the hydrofracturing pressure was examined. When the diameter ratio  $R(=d/d_B)$  was 37.5, d and  $d_B$  were 150 (mm) and 4 (mm) respectively. These results indicate that the effect of the sample size on the hydrofracturing pressure is not necessary to consider. The value of  $(P_{fv}-\sigma_h)$  of sample B was almost equal to the unconfined compression strength of sample B  $(q_u=1.00\sim1.30~(kgf/cm^2))$ .

Therefore, it is concluded that the vertical hydrofracturing pressure  $P_{fv}$  can be given by Eq. (4), irrespective of the sample size.

# HORIZONTAL OR INCLINED HYDROFRACTURE

Haimson and Fairhurt (1970) had pointed out through the hydraulic fracture tests on many kinds of rock samples, "horizontal fracture were initiated only in those samples where a vertical stress concentration, near the end of the pressurized hole, was possible".

However, in the fracture tests of cohesive

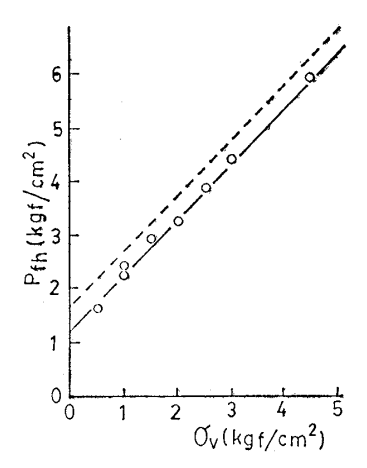


Fig. 10. Horizontal or inclined fracture tests of sample B in  $\sigma_v = \sigma_h - 0.50$  (kgf/cm²): 1 (cp) liquid

The dashed line presents the vertical hydrofracturing pressure given by Eq. (6).  $q_u = 1.20$  (kgf/cm²)

soils, the hydraulic fracture can be seen even in the middle of the sample not only in the end of borehole. The direction of fracture was horizontal or inclined. The horizontal or inclined hydrofracture indicates that the hydrofracture of cohesive soils is not necessarily initiated by tensile failure.

Fig. 10 shows the test results of sample B. The vertical (axial) pressure was smaller than the lateral pressure and the difference was 0.50 (kgf/cm<sup>2</sup>) in these tests. These results indicate that Eq. (5) can be applied to the results. And  $\sigma_a$  was nearly equal to the unconfined compression strength  $q_u$ .

$$P_{fh} = \sigma_v + \sigma_a = \sigma_v + q_u \tag{5}$$

 $\sigma_a$ : the intercept in  $P_{fh}$  axis

The vertical fracture was not seen. The dashed line in Fig. 10 shows the vertical hydrofracturing pressure given by Eq. (6). The reason why the vertical fracture was not generated in these cases is that the fracturing pressure was smaller than the pressure required to arise the vertical hydrofracture.

$$P_{f_v} = \sigma_h + q_u = \sigma_v + q_u + 0.50$$
 (6)

In addition, it should be noted that the horizontal or inclined hydrofracture was unexpectedly seen even in the isotropic stress condition. Fig. 11 shows the test results on

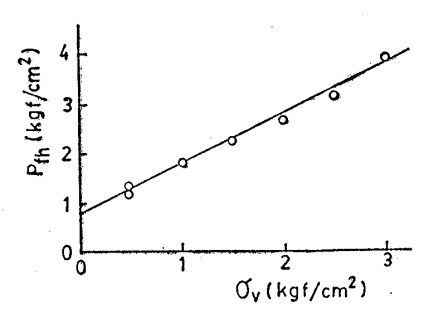


Fig. 11. Horizontal or inclined fracture tests of sample C in isotropic stress condition: 1 (cp) liquid

sample C under the isotropic stress condition demonstrating that the relation between the hydrofracturing pressure  $P_{fh}$  and the vertical pressure  $\sigma_v$  is given by Eq. (5). The possibility of horizontal or inclined hydrofracture increases as the strength  $q_u$  of sample becomes small.

# EFFECT OF PRE-EXISTENT WEDGE AND PRESSURIZING RATE ON HY-DROFRACTURING PRESSURE

In order to clarify the effect of the tensile crack around the borehole on the hydrofracturing pressure, the authors performed the fracture tests on the sample which had the pre-existent wedge. The pre-existent wedge was given by the steel wire before setting the specimen in the fracturing apparatus as shown in Fig. 12. The test results are presented in Table 3. The results indicate that the effect of the pre-existent wedge on the

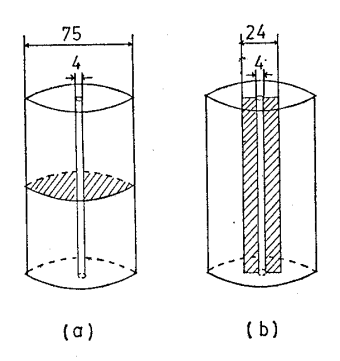


Fig. 12. Pre-existent wedge of sample (a) Horizontal pre-existent wedge (H)

(b) Vertical pre-existent wedge (V)

Sample No.	Pre-existent wedge	$\sigma_v$	$\sigma_k$	η	$P_r$	$q_u$	$D_f$	$P_f$
A	H	1.50	1.00	1	0.0016		Н	1.55
$\mathbf{A}$	H	1.50	1.00	1	0.02	1.40	H or V	2.56
$\mathbf{A}$	H	1.50	1.00	500	0.02		V	2.82
${f A}$	<i>V</i>	1.50	1.00	1	0.02		V	2.28
$\mathbf{A}$	V	1.50	1.00	1	0.02	1.80	v	2.39
· <b>A</b>	without wedge	1.50	1.00	500	0.02		V	2.67
C	. V	0.70	0.50	1	0.02	0.75	V	1.06
<b>C</b> .	V	0.70	0.50	500	0.02	₹	V	1.20
C	without wedge	0.70	0.50	500	0.02	0.83	V	1.20

Table 3. Effect of pre-existent wedge on the hydrofracturing pressure

 $P_r$ : pressurizing rate (kgf/cm²/s),  $D_f$ : Direction of fracture,  $\eta$ : (cp), H: Horizontal, V: Vertical,  $\sigma_v$ ,  $\sigma_h$ ,  $q_u$ ,  $P_f$ : (kgf/cm²) 1kgf/cm²=98kN/m²

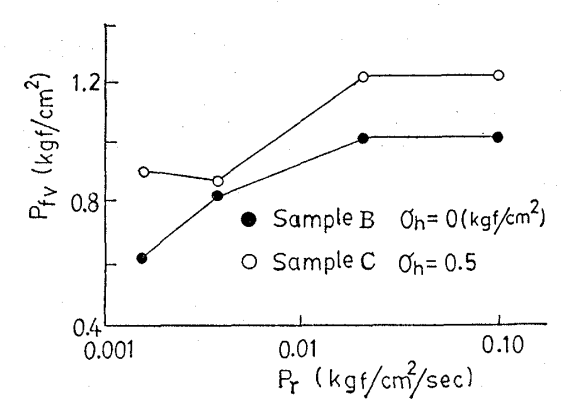


Fig. 13. Effect of pressurizing rate  $P_r$  on the vertical hydrofracturing pressure  $P_{fv}$ : 500 (cp) liquid

hydrofracturing pressure was negligible except when the pressurizing rate  $P_r$  was very slow  $(P_r=0.0016 \, (\text{kgf/cm}^2/\text{s}))$ . Whether or not the hydrofracturing pressure is influenced by the wedge depends upon the degree of liquid penetration into the wedge. Thus the influence would depend upon the width or length of wedge, the viscosity of the liquid, and the pressurizing rate.

Fig. 13 shows the effect of the pressurizing rate on the hydrofracturing pressure. Fig. 14 shows the typical results of the relation between the borehole pressure P and the inflow volume V in the case of sample C. When the pressurizing rate  $P_r$  was slow, the strength of the soil around the borehole would decrease because of swelling or liquid permeation. The tensile crack around the borehole might influence on the hydrofracturing pressure. Therefore,  $P_{fv}$  would decrease as  $P_r$  decreases. As seen in Fig. 13, however, there would be a upper limit of

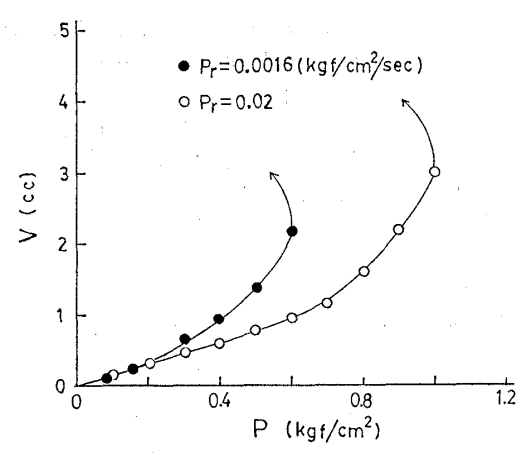


Fig. 14. Effect of the pressurizing rate  $P_r$  on the relation between inflow volume V and borehole pressure P of sample B:500 (cp) liquid,  $\sigma_h=0\,\mathrm{kgf/cm^2}$ 

the hydrofracturing pressure, irrespective of the pressurizing rate.

The hydrofracturing pressure in the fields may be lower than the value given by Eq. (4) or Eq. (5), because the pre-existent wedge may be large enough. Thus the hydrofracturing pressure given by Eq. (4) or Eq. (5) would be the maximum value as long as the viscosity and the pressurizing rate are of ordinary ones.

# HYDROFRACTURE CRITERIA OF CO-HESIVE SOILS

Through the previous sections, the authours suggested that the hydrofracturing pressure  $P_f$  is given by Eq. (7), irrespective of the direction of fracture surface.

$$P_f = \sigma_{\min} + q_u \tag{7}$$

 $\sigma_{\min}$ : the minimum principal stress

21

The hydraulic fracture of cohesive soils is not necessarily initiated by tensile failure, since the horizontal or inclined fracture was initiated in some cases.

The shear failure criteria given by the radial stress  $\sigma_r$  and the tangential normal stress  $\sigma_{\theta}$  is:

$$\sigma_r - \sigma_\theta = q_u \tag{8}$$

As, in elastic theory, the shear failure around the borehole would be initiated when the borehole pressure P reaches  $P_{fve}$  (= $\sigma_h$ + $q_u$ /2), the hydrofracturing pressure  $P_{fv}$  is larger than  $P_{fve}$ . The initiation of hydrofracture might require the shear failure to some extent near the borehole. The intermediate principal stress  $\sigma_v$  might add some more pressure to the pressure  $P_{fve}$  given by Eq. (8), for Eq. (8) disregards the effect of  $\sigma_v$  on the shear strength.

In addition, the following explanation might be possible. Assume that the tensile strength of the sample is the value determined in Brazilian test, then the tensile crack around the borehole may be generated when the borehole pressure P reachs  $(\sigma_h + \sigma_t)$ . It should be noted that the tensile strength  $\sigma_t$  is determined as the total stress. But the liquid in the borehole probably could not penetrate into the crack when the pressurizing rate is high enough, because the effect of tensile wedge around the borehole on the hydrofracturing pressure is negligible as shown in Table 3.

If the tangential normal stress could not exceed the tensile strength, Eq. (9) is suggested in terms of total stress, because all tests were performed in unconsolidated condition.

$$\sigma_{\theta} > = \sigma_h - \sigma_t \tag{9}$$

Therefore the minimum radial stress required to initiate the shear failure around the borehole is given by Eq. (10).

$$\sigma_r = \sigma_h + q_u - \sigma_t \tag{10}$$

Eq. (10) becomes Eq. (11), for the ratio of  $\sigma_t$  to  $q_u$  is generally  $(1/5 \sim 1/6)$  in cohesive soils (Nishigaki, 1979).

$$\sigma_r = \sigma_h + (0.80 \sim 0.84) q_u$$
 (11)

The shear failure criteria given by the radial stress  $\sigma_r$  and the vertical axial stress  $\sigma_v$  is:

$$\sigma_r - \sigma_v = q_u \tag{12}$$

The radial stress  $\sigma_r$  given by Eq. (11) and Eq. (12) are nearly equal to the hydrofracturing pressure, because  $\sigma_r$  around the borehole is equal to the borehole pressure P.

Therefore, it would be the shear failure near the borehole—rather than the tensile failure—which initiate the hydraulic fracture of cohesive soils, irrespective of the direction of the fracture surface. This fracture mechanism seems to be reasonable, especially in case of the horizontal or inclined hydrofracture.

In the cases of rock and concrete, the hydrofracturing pressure when  $\sigma_h=0$  is considerably smaller than  $q_u$ . The hydrofracture of them would be initiated by the tensile failure rather than the shear failure. ever, the tensile crack in cohesive soils, the strength of which is much smaller than the rock and concrete, would generally grow as the closed crack unless the soil is very brittle. Thus it is deduced that the liquid in the borehole could not penetrate into the crack untill the shear failure around the borehole is generated. The hydrofracturing pressure given by Eq. (7) is the maximum value in the cases of cohesive soils as long as the viscosity of the liquid and the pressurizing rate are of ordinary ones.

The hydrofracture after the liquid penetrates into the crack is progressed by the wedge action. And the direction of fracture is generally normal to the direction of the minimum principal stress, because the liquid penetrates into the direction easily.

# CONCLUSIONS

Through the test results on six kinds of cohesive soils, it was found that the hydrofracturing pressure is given by Eq. (7) in terms of total stress, irrespective of the direction of fracture surface. The possibility of the horizontal or inclined hydrofracture to take place increases as the unconfined strength of the sample becomes smaller.

The viscosity of the liquid in the borehole and the size of sample have little influence on the hydrofracturing pressure as far as the pressurizing rate is high enough.

It is the shear failure near the borehole—rather than the tensile failure—, which initiates the hydraulic fracture in cohesive soils, because the effect of the tensile crack on the hydrofracturing pressure seems to be negligible as long as the liquid can not penetrate into the crack.

### **ACKNOWLEDGEMENTS**

The authors wish to express their gratitude to K. Sato and K. Haraguchi for experimental details and to Mr. N. Yokoyama for technical assistances.

#### REFERENCES

- 1) Bjerrum, L., Nash, J. K. T. L., Kennard, R. M. and Gibson, R. E. (1972): "Hydraulic fracturing in field permeability testing," Géotechnique, Vol. 22, pp. 319-332.
- 2) Massarsch, K. R. and Broms, B. B. (1977): "Fracturing of soil caused by pile driving in clay," Proc. 9th Int. Conf. on Soil Mech. and Found. Eng., Vol. 1, 1977, pp. 197-200.
- 3) Morgenstern, N. R. and Vaughan, P. R. (1963): "Some observations on allowable grouting pressure," Grouts and Drilling Muds in Engineering Practice, London, Butterworths, pp. 36-42.
- 4) Hubbert, M. K. and Willis, B. G. (1957): "Mechanics of hydraulic fracturing," Trans. AIME, 210, pp. 153-166.

- 5) Haimson, B. and Fairhurt, C. (1967): "Initiation and extention of hydraulic fractures in rocks," Soc. Petrol. Eng. J., 7, pp. 310-318.
- 6) Haimson, B. and Fairhurt, C. (1970): "In-situ stress determination at great depth by means of hydraulic fracture," Proc. 11 th Symp. Rock Mech., AIME, pp. 559-584.
- 7) Zoback, M. D., Rummel, F., Jung, R. and Raleigh, C. B. (1977): "Laboratory hydraulic fracturing experiments in intact and pre-fractured rock," Int. J. Rock Mech. Min. Sci. & Geomech. Abstr., Vol. 14, pp. 49-58.
- 8) Ishizima, Y., Kinoshita, S., Ito, Y. and Machida, K. (1980): "Experimental study on hydrofracturing stress measurements," Journal of the Mining and Metallurgical Institute of Japan, Vol. 96, No. 1114, pp. 871-877 (in Japanese).
- 9) Harada, T., Idemitsu, T. and Watanabe, A. (1985): "Demolition of concrete with expansive demolition agent," JSCE; No. 360, pp. 61-71 (in Japanese).
- 10) Lockner, D. and Byerlee, J. D. (1977): "Hydro-fracture in weber sand stone at high confining pressure and differential stress," Journal of Geophysical Research, Vol. 82, No. 14, pp. 2018-2026.
- 11) Jaworski, G. W., Duncan, J. M. and Seed, H. B. (1981): "Laboratory study of hydraulic fracturing," Proc. ASCE, GT 6, pp. 713-732.
- 12) Vesic, A. S. (1972): "Expansion of cavities in infinite soil mass," Proc. ASCE, SM 3, pp. 265-290.
- 13) Massarsch, K. R. (1978): "New aspects of soil fracturing in clay," Proc. ASCE, GT8, pp. 1109-1123.
- 14) Nishigaki, K. (1979): Soil Mechanics and Foundation Engineering Library 4, JSSMFE, pp. 182-183.